

UTILIZATION OF AN sUAS-BASED THERMAL CAMERA TO DETERMINE RELATIVE THERMAL INERTIA OF VOLCANIC DEPOSITS. B. B. Carr¹, K. A. Bennett², E. Lev¹, and C. S. Edwards³, ¹Lamont-Doherty Earth Observatory, Columbia University, 61 Route 9W, Palisades, NY 10964, bcarr@ldeo.columbia.edu, ²USGS Astrogeology Science Center, 2255 N. Gemini Dr., Flagstaff, AZ 86001, ³Department of Physics and Astronomy, Northern Arizona University, NAU Box 6010, Flagstaff, AZ 86011-6010.

Introduction: In this study, we investigate the thermophysical properties of volcanic deposits using a small unmanned aerial system (sUAS) carrying a thermal infrared camera. We repeated a mapping survey with the sUAS and thermal camera to generate a time series of temperature maps of an area near the summit of Sierra Negra Volcano, Ecuador. The surveyed area contains a variety of volcanic deposits including both pahoehoe and a'a lava flows, tephra, and vents from an eruption in June 2018. The repeat surveys allow us to measure the rate of heating for these various volcanic surfaces induced by solar input, which we use as a relative measure of thermal inertia to infer relative physical properties of the deposits.

Thermal inertia is a physical material property that measures resistance to an external change of temperature [1]. The thermal inertia of a land surface is commonly used to investigate Martian surfaces, where the value can provide information on the degree of mantling by dust and the presence of exposed bedrock [1,2]. For terrestrial targets, the earth's thick atmosphere and vegetation can complicate direct measurement of thermal inertia, but an "apparent thermal inertia" value can be derived from satellite measurements and be used to investigate, for example, soil moisture [3] and mantling of lava flows [4]. In general, lower thermal inertia is associated with finer-grained material (such as dust) while higher thermal inertias correspond to larger particle sizes or bedrock [1,2,4]

Using thermal inertia (and remote sensing techniques in general) provides a means to investigate the physical properties of planetary surfaces when these areas are not accessible for direct ground-based field measurements, such as active volcanic environments or Martian surfaces. Additionally, remote sensing can provide reconnaissance and context mapping as part of more detailed or localized field studies. Combining high resolution thermal inertia measurements with ground truthing of surface characteristics, as done in this study, thus allows for improved interpretation of thermal inertia measurements and better understanding of planetary surface processes.

Sierra Negra is a basaltic shield volcano located on Isla Isabela in the Galápagos Archipelago (Fig. 1a). The 2018 eruption of Sierra Negra began on June 26, when multiple fissures opened near the summit and generated multiple lava flows up to 7 km long [5]. Lava from these vents initially had pahoehoe texture and then

transitioned to a'a within a few hundred meters (Fig. 1b). Following the initial June 26 activity, the eruption moved downslope (northwest), where a sustained vent was active from June 27 through August 23 [5].

Methods: We use a DJITM Matrice 210 sUAS mounted with a Zenmuse X4S visual camera (20 MP resolution, 24 mm focal length) and a Zenmuse XT thermal camera (640x512 resolution, 13mm focal length) to capture the images used for this study. We flew the sUAS three times on the morning of October 22, 2018, at 07:15, 08:30, and 09:45 to capture the solar heating of the ground surface. Fog prevented a pre-dawn flight, but also minimized solar heating until clouds cleared enough to allow sUAS flight. Flights averaged 24

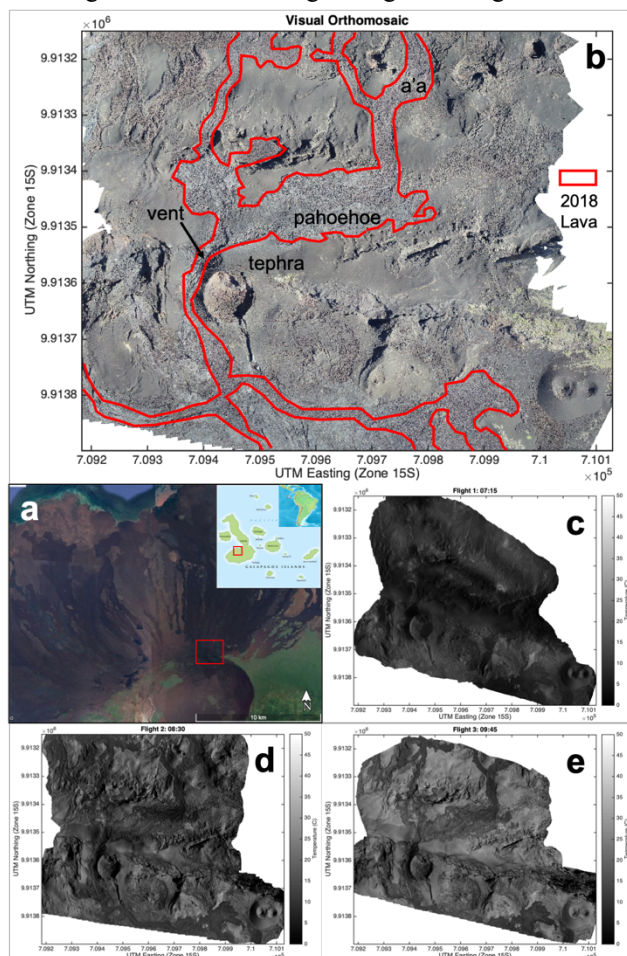


Figure 1. Location of Sierra Negra Volcano (a) and the study area; a sUAS-derived visual orthophoto of the study area is shown in (b). Temperature maps from 3 sUAS flights (c, d, e) show variable rates of solar heating.

minutes in length with 450 images from each flight.

We linearly scale the thermal images from each flight to convert from temperature to 16-bit digital number (DN), which enables the images to be processed by photogrammetry software. We use Agisoft Photoscan Pro™ to align the thermal images and generate a 3D model of the surveyed terrain for each flight. The GPS position from the sUAS attached to each image is used to provide spatial reference for the models. From the model, we export a 2D orthomosaic, which we convert back to temperature in Matlab™. Each orthomosaic has a resolution of 0.2 m.

We estimate the rate of heating for each pixel in the temperature maps by calculating the slope of the best fit line for the temperature values for each pixel in the three images. In future work, we will eliminate all pixels where the ground surface slope exceeds 20 degrees to minimize the effects of shadows and solar incidence angle. Slope was calculated from a DEM of the survey area created in Photoscan using visual images from the second sUAS flight. We also use these visual images to generate a 4 cm orthophoto of the survey area (Fig 1b).

Results: The visual orthophoto shows the variety of volcanic deposits in the study area (Fig. 1b) and identifies the lava flow from the June 26 vent. The temperature maps from the three flights (Figs. 1c, 1d, 1e) show variable magnitudes of solar heating in the 2.5 hours between the first and last flights. The brightest (hottest) locations in Figs. 1c-1e are where heat is escaping from the still-cooling lava flows. In individual thermal images, single pixel temperatures exceeded 100 °C.

The slope of the best fit line through the temperature values for each pixel from the three maps (Fig. 1c-e) is shown as the rate (°C per hour) of heating in Fig. 2. Distinct differences between a'a, pahoehoe, and tephra

surfaces can be identified. Tephra shows the faster heating rate and a'a a slower rate, with pahoehoe in between. This is a similar trend to that observed using satellite-derived apparent thermal inertia, which showed that smaller particle sizes (i.e. tephra deposits) have a lower thermal inertia (i.e. faster heating rate) compared to larger particle sizes (i.e. the blocky surface of an a'a lava flow) [1].

Future work will investigate the results shown in Fig. 2 for variations in heating rate of the lava flows in both down-flow and cross-flow directions, and variations in tephra deposits with distance from the vent.

Discussion: This study demonstrates a new method for using sUAS data to study volcanic phenomena, but is broadly applicable to many planetary surfaces. The use of sUAS for this study also produces much higher resolution relative thermal inertia data products compared to previous works using satellite thermal images (compare 0.2 m pixel size in this study to 90 m pixel size for the ASTER instrument used in [3,4] or 100 m pixel size for the THEMIS instrument used in [2]). Thermal inertia studies from terrestrial sUAS surveys may also aid mission planning and interpretation of data from the sUAS on the Mars2020 rover.

This technique also enables use of thermal inertia measurements to investigate surface morphology. As field work was conducted only 4 months after the eruption, negligible mantling or erosion has occurred. Thus, the variability of relative thermal inertia in Fig. 2 is directly due to changes in the thermophysical properties of the deposits themselves and, combined with the high spatial resolution of the data, can provide detailed information on the morphology and rheology of the lava flows and the distribution of tephra around the vent. The presence of deposits from previous eruptions will also allow for comparison between similar deposits of different age.

References: [1] Ramsey M. S. et al. (2016) *JVGR*, 311, 198-216. [2] Fergason R. L. et al. (2006) *JGR*, 111, E12004. [3] Scheidt S. et al. (2010) *JGR*, 115, F02019. [4] Price M. A. et al. (2016) *Remote Sens.*, 8, 152. [5] Ruiz M. C. et al. (2018) *AGU Fall Meeting*, Abstract #V31C-02.

Acknowledgements: This work is supported by NSF EAR Postdoctoral Fellowship Award #1725768 and a WHOI Independent Research and Development Grant (PI: Adam Soule). EL was supported by NSF award EAR-1654588.

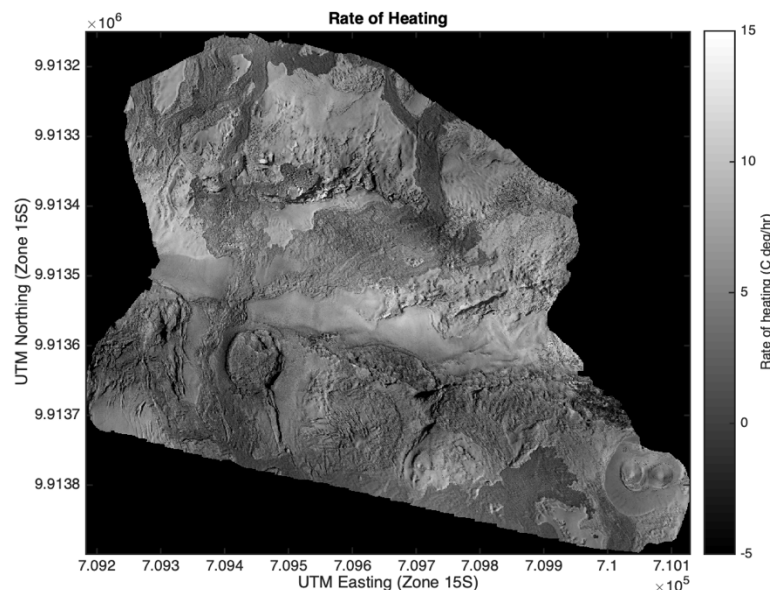


Figure 2 (left). Rate of heating for the study area calculated from the 3 temperature maps (Fig. 1c-e).